Axial Response of Three Vibratory- and Three Impact-Driven H Piles in Sand

JEAN-LOUIS BRIAUD, HARRY M. COYLE, AND LARRY M. TUCKER

Three H piles were impact driven in a medium dense sand deposit, load tested in compression, and then extracted. The same three piles were then vibro-driven at a different location and load tested in compression. The top load-top movement curves show that the vibro-driven piles have, on the average, the same ultimate capacity as the hammer-driven piles. These curves also show that at half the ultimate load, the movement of the vibro-driven piles is 2.5 times larger than the movement of the hammer-driven piles, on average. At half the ultimate load, however, the movement of the vibro-driven piles was only 0.25 in. Some of the piles were instrumented; this allowed researchers to obtain the load transfer curves. These curves showed that the vibro-driven piles carry much more load in friction and much less load in point resistance than the hammer-driven piles.

In the spring and summer of 1986, a series of vertical load tests was carried out on instrumented piles driven in sand at Hunter's Point in San Francisco. The Federal Highway Administration (FHWA) sponsored two projects on impact-driven piles: one on the testing of five single piles, and one on the testing of a five-pile group (*1,2*). The U.S. Army Engineer Lower Mississippi Valley Division (LMVD), Waterways Experiment Station (WES), and FHWA then sponsored a project on the comparison of impact-driven piles and vibratory-driven piles. Subsequently, the Deep Foundation Institute drove a number of piles with various vibratory hammers to compare the hammers' efficiencies.

This article is a summary analysis of the pile load tests sponsored by LMVD, WES, and FHWA comparing impact- and vibratory-driven piles. The site is characterized, the load tests are described, the load tests results are analyzed and discussed, and conclusions are made. The details of the work can be found in Tucker and Briaud (*3*).

THE SOIL

The soil has been described in detail by Ng, Briaud, and Tucker (*1*). Below a 4 in. thick asphalt concrete pavement is a 4.5 ft thick layer of sandy gravel with particles up to 4 in. in size. From 5 ft to 40 ft depth is a hydraulic fill made of clean sand (SP). Below 40 ft, layers of medium stiff to stiff silty clay (CH) are interbedded with the sand down to the bedrock. The fractured serpentine bedrock is found between 45 ft to 50 ft depth. The water table is 8 ft deep.

Department of Civil Engineering, Texas A&M University, College Station, Tex. 77843.

Many tests have been performed at the site, including standard penetration tests (SPTs) with a donut hammer and a safety hammer, sampling with a Sprague-Henwood sampler, cone penetrometer tests (CPTs) with point, friction and pore pressure measurements, preboring and selfboring pressuremeter tests, shear wave velocity tests, dilatometer tests, and stepped-blade tests. The CPT, SPT, and stepped-blade tests were performed before and after driving and testing of the FHWA test piles. Selected profiles are shown in Figures 1 through 6. The hydraulic fill has the following average properties: friction angle 32 to 35 degrees, water content 22.6 percent, dry unit weight 100 pcf, D_{60} 0.8 mm, D_{10} 0.7 mm, SPT blow count 15 bpf, CPT tip resistance 65 tsf, PMT net limit pressure 7 tsf, and shear modulus (from shear wave velocity measurements) 400 tsf.

THE PILES AND THE LOAD TESTS

Three HP14x73 steel H piles were used in this program. They were all embedded 30 ft below the ground surface; however, a 4.5 ft deep, 14 in. diameter hole was drilled prior to pile insertion for the impact driven piles, making the true pile embedment equal to 25.5 ft. For the vibratory-driven piles a hole was drilled through the 4 in. thick asphalt layer only, making the embedment equal to 29.5 ft. Each pile had two angles (2.5 x 2.5 x 3/16 in.) welded to the sides of the pile web as protection for the instrumentation.

The first pile (Pile 1) was one of the single piles used in the FHWA program. Pile 1 was instrumented with seven levels of strain gauges and a telltale at the pile tip. This pile was calibrated before driving and the pile stiffness was measured for use in the data reduction. The measured value of pile stiffness (AE) was 614,908 kips. This value was used for all three piles. Pile driving analyzer measurements were obtained during the driving of Pile 1 with an impact hammer. Pile 1 was then load tested in compression 30 days after it was driven (FHWA program): this is load test 1I. Pile 1 was then retested at 67 days after driving: this is load test 1IR. After Pile 1 was retested, the pile was restruck with an impact hammer and pile driving analyzer measurements were obtained. Pile 1 was then extracted and vibro-driven about 30 ft from the impact test. It was load tested at 33 days after driving (load test 1V) and again at 63 days after driving (load test 1VR). After load test 1VR the pile was struck with an impact hammer and pile driving analyzer measurements were obtained.

The second pile (Pile 2) was instrumented with two levels of strain gauges: one at the point and one at mid-length. Pile 2 was impact driven and tested at 65 days after driving: this is load test 2I. Pile 2 was then extracted and vibrodriven and

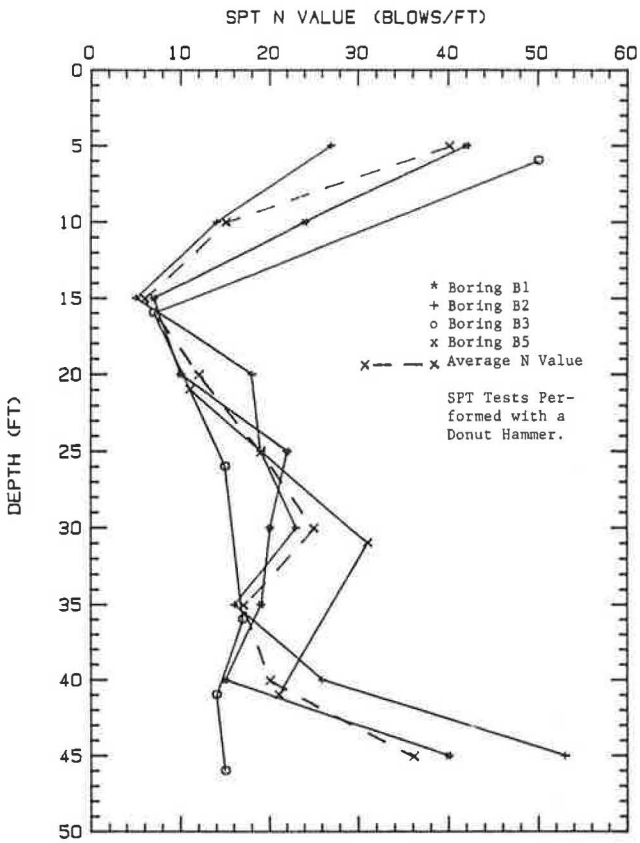

FIGURE 1 Profiles of standard penetration test blow counts.

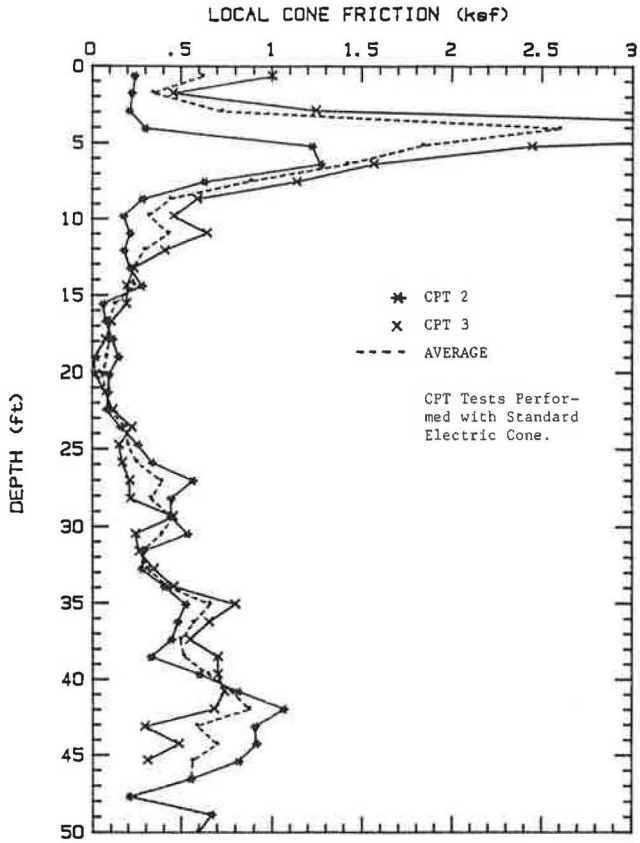

FIGURE 3 Cone tip penetration test profiles for friction resistance.

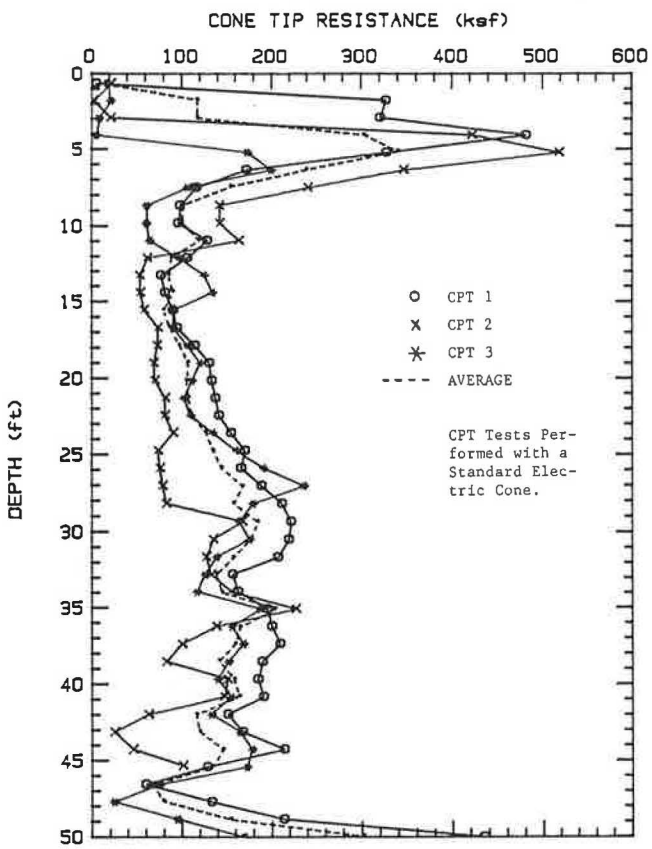

FIGURE 2 Cone tip penetration test profiles for point resistance.

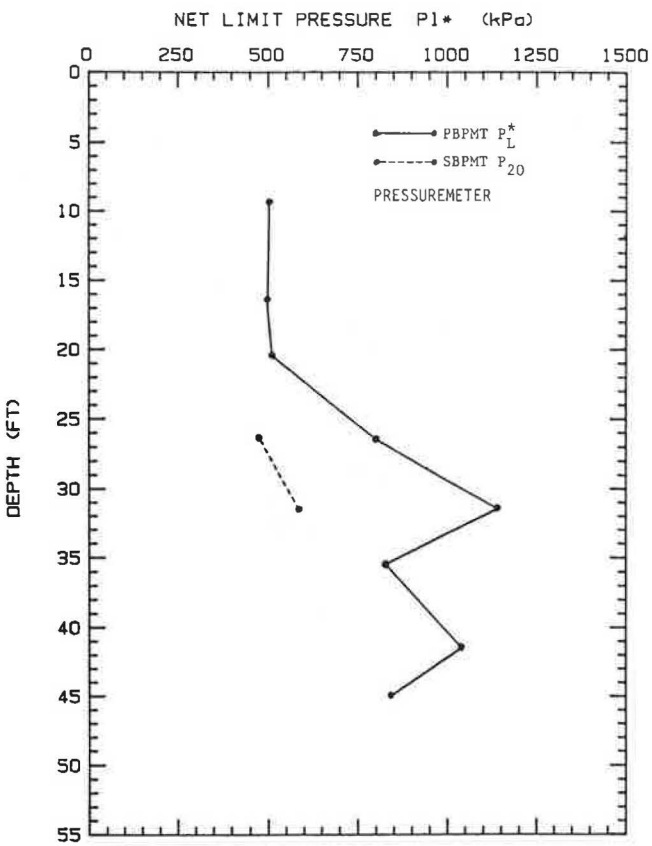

FIGURE 4 Net limit pressure profile.

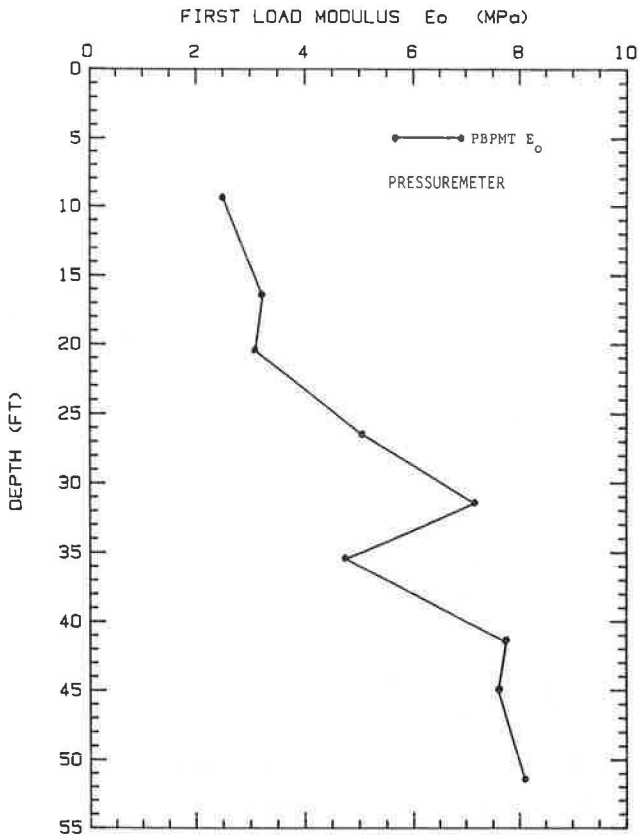

FIGURE 5 First load modulus profile.

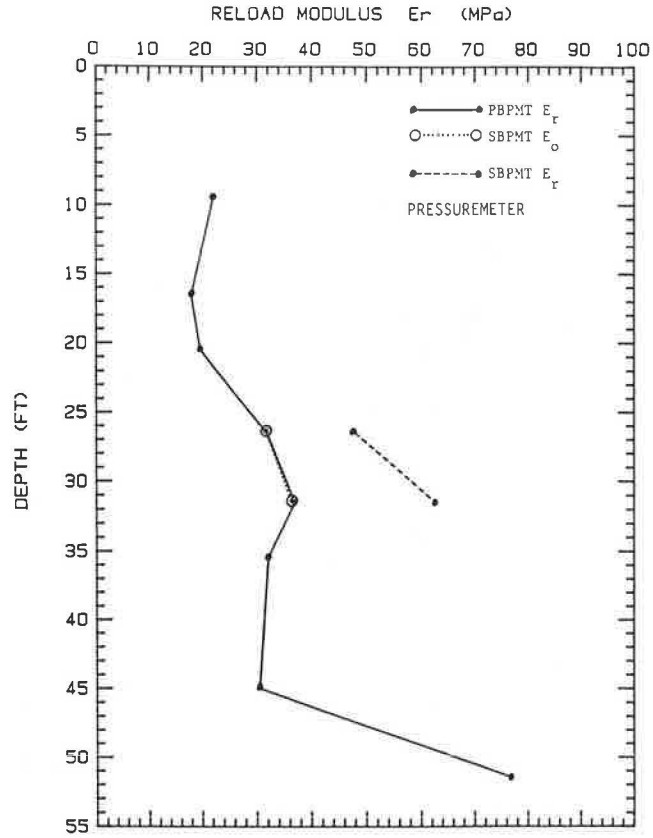

FIGURE 6 Reload modulus profile.

tested at 64 days after driving. This is load test 2V. After load test 2V, the pile was struck with an impact hammer and pile driving analyzer measurements were obtained.

The third pile (Pile 3) was not instrumented. It was impact driven and tested at 12 days after driving: this is load test 3I. Pile 3 was then extracted and vibrodriven. It was tested at 12 days after driving: this is load test 3V. Table 1 summarizes the eight load tests presented in this report.

The impact-driven piles were installed using a Delmag D22 diesel hammer at full throttle. All restrike measurements were also obtained using this hammer. The final blow count for the impact driven piles averaged 11.5 blows/ft (Table 2). The specifications for the Delmag D22 hammer are given in Table 3.

The vibratory-driven piles were installed with an ICE-216 vibratory hammer (Table 4). The penetration rate over the last 2 ft of penetration varied between 12 and 20, averaging 16 ft/min (Table 2). The impact hammer and the vibratory hammer drove the piles in approximately the same time.

The load test procedure consisted of applying the load of 10 percent of the estimated ultimate load. Each load step was held for at least 30 minutes, with the load being monitored continuously. All readings from electronically monitored instruments were recorded every 5 minutes.

RESIDUAL STRESSES

Residual driving stresses were measured for Pile 1I. The stress profile was not monitored between load test 1I and test 1IR. Therefore the same residual stress profile after driving was also used for load test 1IR. Since additional residual stresses are usually induced due to a compression test, this profile and all subsequent profiles for Pile 1R are in error by an unknown amount. The residual stress profile is the first load profile shown in Figure 7.

An attempt was made to record the residual driving stresses for Pile 2I. However, the readings obtained were judged unreliable. Therefore, the residual stress profile from Pile 1I was used in reducing the load test data for Pile 2I (Figure 7).

The vibratory-driven piles were assumed to have no residual driving stresses. No attempt was made to verify this. However, published data substantiate this assumption (*4*).

LOAD TEST RESULTS

The load movement curves for all the piles are shown on Figure 8. The point load-point movement curves backfigured from the measured data are presented on Figure 9. The load versus depth profiles for Piles 1I and 1V are presented on Figures 7 and 10, respectively. The friction transfer curves were obtained after fitting the load versus depth profiles with a second order polynomial curve. The friction transfer curves are shown for Piles 1I and 1V in Figures 11 and 12, respectively.

PILE DRIVING ANALYZER RESULTS

The pile driving analyzer (PDA) consists of the dynamic monitoring of strain gauges and accelerometers attached to the

TABLE 1 LOAD TEST PROGRAM SUMMARY

Test Piles		
1I	- FHWA Pile (Impact)	30 Day Test
1IR	- FHWA Pile (Impact)	67 Day Test
1V	- FHWA Pile (Vibratory)	33 Day Test
1VR	- FHWA Pile (Vibratory)	63 Day Test
2I	- New Pile (Impact)	65 Day Test
2V	- New Pile (Vibratory)	64 Day Test
3I	- New Pile (Impact)	12 Day Test
3V	- New Pile (Vibratory)	13 Day Test

Notes:

A. 1I, 1IR, 1V, and 1VR - Seven strain gauge levels

B. 2I and 2V - Two strain gauge levels

C. 3I and 3V - No strain gauges

TABLE 2 DRIVING RECORDS

		Pile 1	Pile 2	Pile 3
Impact Driven	- last foot	12 bl/ft	NA	11 bl/ft
	- total	96 blows	NA	131 blows
Vibro-Driven	- last foot	20 ft/min	15 ft/min	12 ft/min
	- total	85 sec.	96 sec.	85 sec.

TABLE 3 SPECIFICATIONS FOR DELMAG D22 IMPACT HAMMER

Rated energy	39,700 ft-lbs
Ram weight	4,850 lbs
Blows/minute	42-60
Maximum explosive pressure on pile	158,700 lbs
Working weight	11,275 lbs
Drive Cap weight	1,500 lbs

TABLE 4 SPECIFICATIONS FOR ICE-216 VIBRATORY HAMMER

Eccentric moment	1000 in-lbs
Frequency	400-1600 vpm
Amplitude	1/4-3/4 inches
Power	115 HP
Pile clamping force	50 tons
Line pull for extraction	30 tons
Suspended weight with clamp	4825 lbs
Length	47 inches
Width	16 inches
Throat width	12 inches
Height with clamp	78 inches
Height without clamp	68 inches

pile close to the top. The strain measurements are used to obtain force measurements as a function of time, and the accelerometer measurements are integrated to obtain velocity versus time. From these two measurements, various parameters may be calculated, including the maximum energy delivered to the pile and the static resistance of the pile by the CASE method. This static resistance represents the PDA capacity prediction.

PDA measurements were made on Pile 1I (driven with the impact hammer) for both the initial driving and the restrike sequence after the load tests were performed, and on Piles 1V and 2V (driven with the vibratory hammer) for restrike after the load tests were performed. The results are presented in Table 5.

DISCUSSION OF RESULTS

Top Load-Movement Curves

The top load-movement curves for the eight load tests are shown together in Figure 8. Two main observations can be made. First, in all cases the vibratory-driven piles have a lower initial stiffness than the impact-driven piles. Second, the impact-

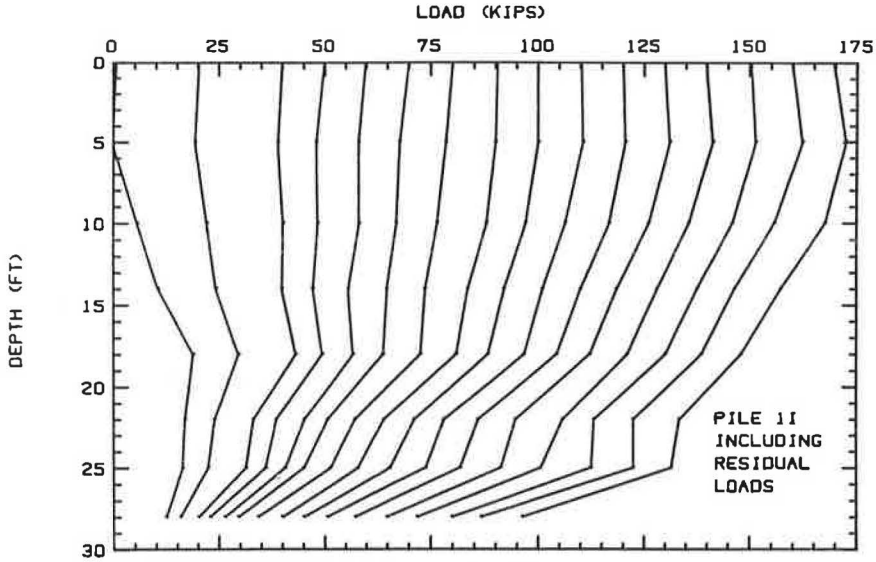

FIGURE 7 Corrected load versus depth profiles for Pile 1I.

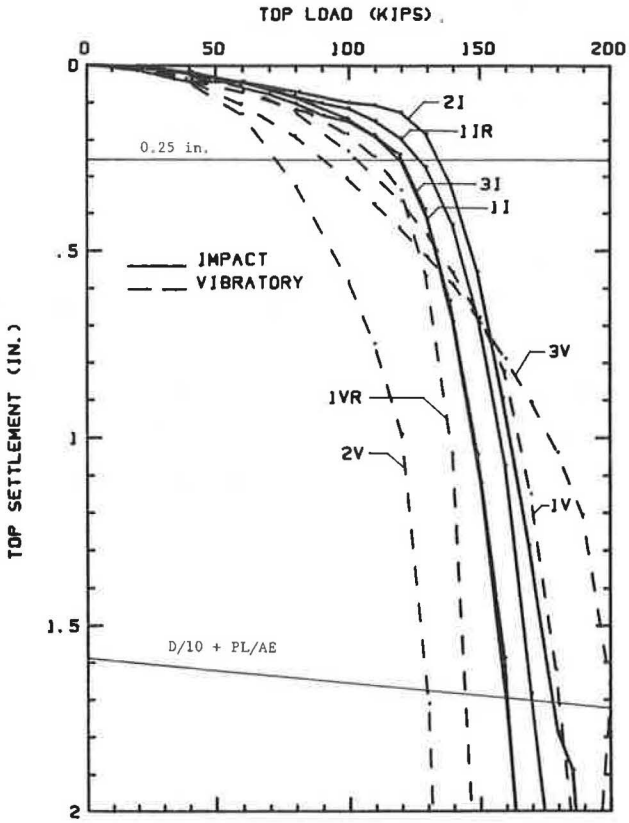

FIGURE 8 Comparison of load-settlement curves.

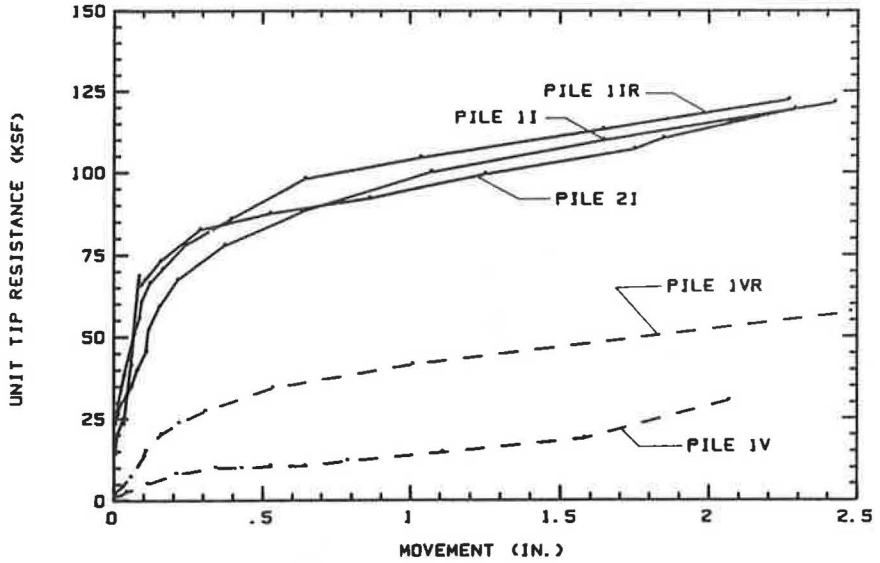

FIGURE 9 Comparison of point load transfer curves.

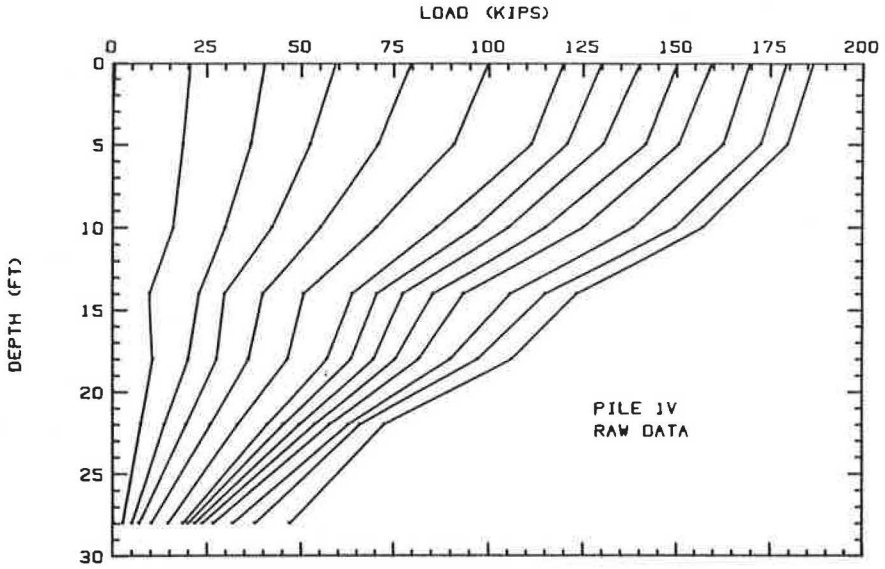

FIGURE 10 Raw load versus depth profiles for Pile 1V.

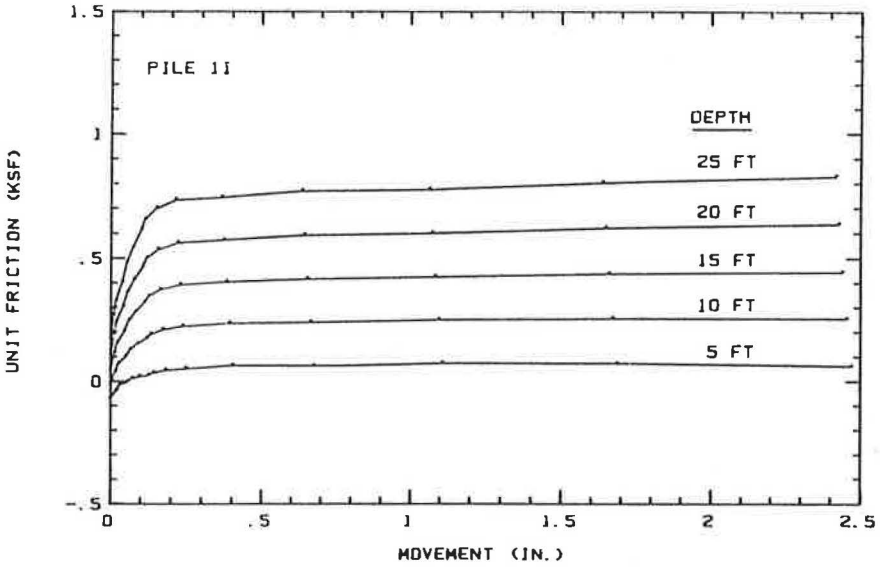

FIGURE 11 Friction versus movement curves for Pile 1I.

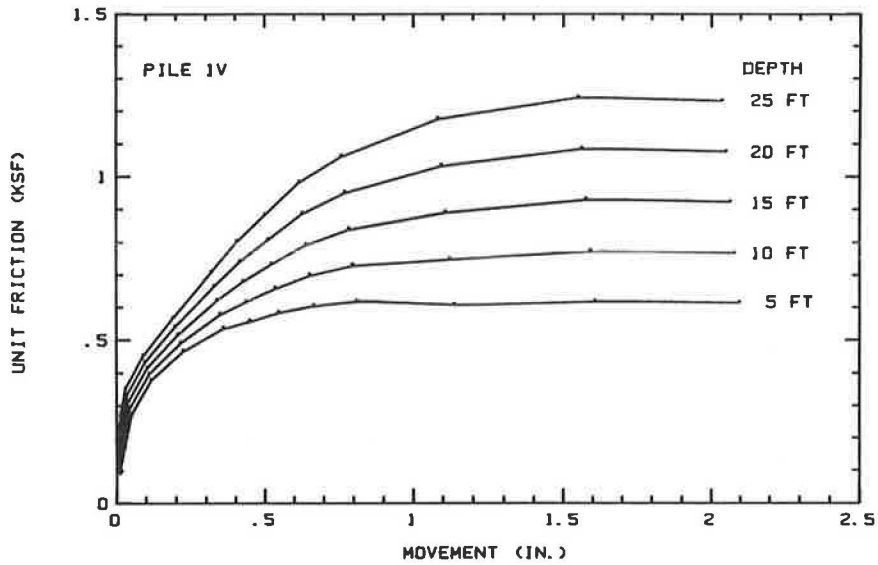

FIGURE 12 Friction versus movement curves for Pile 1V.

TABLE 5 PILE DRIVING ANALYZER RESULTS (7)

Pile	Blowcount	Maximum Force (kips)	Maximum Energy (kip-ft)	Estimated Capacity[a] (kips)
1I[b]	12/12 in.	340-510	5-15	140-165
1I[c]	6/6 in.	350-505	10-17	145-200
1V[c]	7/6 in.	300-415	4-13	120-140
2V[c]	14/12 in.	355-520	5-11	125-150

[a]Case method capacity assumes a damping constant $J = 0.25$.
[b]Initial driving.
[c]Restrike.

driven piles show more consistent response between piles than the vibratory-driven piles. Third, on the average, the ultimate load is the same for the vibro-driven and the impact-driven piles, but the ultimate load is more erratic for the vibro-driven piles.

In an effort to quantify these observations, four measurements have been made from the load-movement curves. First, the ultimate load has been defined as the load corresponding to a movement of one-tenth of the equivalent pile diameter plus the elastic compression of the pile under that load as if it acted as a free-standing column. This line has been drawn on Figure 8. Second, the load at a movement of 0.25 in. has been obtained from the load-movement curves. Third, the movement at one-half the defined ultimate load has been obtained. Fourth, the piles' stiffness response has been calculated as one-half the defined ultimate load divided by the movement occurring at that load. These four items are tabulated in Table 6 for the eight load tests.

Table 6 shows that, on the average, there is only 1 percent difference in the average ultimate load between the impact-driven piles and the vibratory-driven piles. However, the coefficient of variation of the ultimate loads for the vibratory-driven piles is 4.3 times higher than that of the impact-driven piles. The factor of safety would therefore have to be higher for the vibro-driven piles in order to obtain the same risk level as for the hammer-driven piles.

The second column of Table 6 shows that at a movement of 0.25 in. the impact-driven piles carry 33 percent more load than the vibratory-driven piles. The coefficient of variation of this load for the vibratory-driven piles is 4.2 times higher than that of the impact-driven piles.

The movement at one-half the ultimate load for the vibratory-driven piles is over two times larger than that of the impact-driven piles, and the coefficient of variation is 5.5 times larger. The movements, however, are very small even for the vibro-driven piles.

The initial stiffness response of the pile, defined as one-half the ultimate load divided by the movement at that load, is 1.91 times higher for the impact-driven piles than for the vibratory-driven piles. The coefficient of variation of this stiffness for the vibratory-driven piles is 3.6 times that of the impact-driven piles.

Load Distribution

The load distribution of the vibratory-driven piles differs greatly from that of the impact-driven piles. At the maximum load, the impact-driven piles carried approximately 51 percent of the load in point resistance, whereas the vibratory-driven piles carried only 13 percent of the load in point resistance (see for example Figures 9, 11, and 12). In the reload test on the vibratory-driven pile, the point resistance had increased to 29 percent of the total load. This indicates that the difference in the driving process causes a different soil reaction, but the difference becomes less upon repeated loading. Indeed, one compression load test can be considered as a slow blow.

The unit friction profiles at maximum loading are shown in Figure 13 for the five instrumented pile tests. Again it can be seen that there is a definite difference in soil reaction between the impact-driven and vibratory-driven piles, and that the difference becomes less pronounced upon repeated loading.

Load Transfer

The H pile presents a problem when computing unit point resistance and unit friction values. What is the failure surface?

TABLE 6 ANALYSIS OF PILE TEST RESULTS

Pile	Load at D/10 + PL/AE (kips)	Load at 0.25 in. (kips)	Movement at $Q_{ult}/2$ (in.)	Initial Stiffness (kips/in.)
1I	160	120	0.104	769
1IR	170	126	0.094	904
2I	175	131	0.088	994
3I	160	120	0.088	909
Average	166	124	0.094	894
Standard Deviation	7.5	5.3	0.0075	93
Coefficient of Variation	0.045	0.043	0.081	0.104
1V	180	102	0.181	497
1VR	145	110	0.103	704
2V	130	71	0.184	353
3V	200	90	0.313	319
Average	164	93	0.195	468
Standard Deviation	32	17	0.087	175
Coefficient of Variation	0.195	0.182	0.446	0.374
Impact / Vibratory	1.01	1.33	0.48	1.91

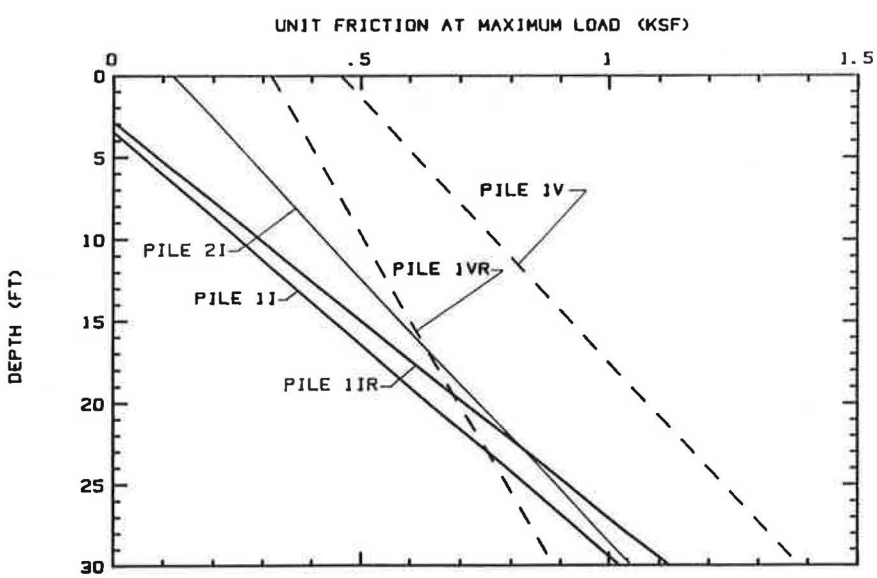

FIGURE 13 Friction versus depth profiles.

One possible assumption is that the pile fails along a rectangle which encloses the H section, with a soil plug forming between the flanges. Another possibility is that the pile fails along the soil-pile interface, with no soil plug forming. Previous research has shown that a better assumption may be that the failure surface is in between the previous two assumptions, with a soil plug filling half the area between the flanges (*1*). For the HP14x73 piles used in this study, this assumption gives the following properties: perimeter, 70.47 in.; tip area, 109.8 in.^{2}. This assumption is used for all further analyses.

Figure 9 shows the unit tip resistance versus tip movement curves for the five instrumented piles. Figure 14 shows the same curves with the tip resistance normalized by dividing by the maximum tip resistance. These two figures show a fundamentally different reaction between the vibratory-driven piles and the impact-driven piles: the tip resistance of the vibratory-driven piles is much lower than that of the impact-driven piles, and the initial slope of the curve is different. However, the difference in shape almost vanishes upon reloading.

The shape of the tip resistance curve of the initial loading of the vibratory-driven pile suggests that the sand immediately under the pile point is initially loose but densifies as the pile is loaded. Indeed, at higher loads the tip resistance begins to increase at a faster rate, rather than reaching a limiting value as the other tests show. By comparing the curves for tests 1I and 1IR, it can be seen that the impact-driven piles do not undergo such a change in behavior between initial loading and reloading.

Figures 15 and 16 show the normalized friction movement curves for the impact-driven piles and vibratory-driven piles, respectively. Figure 15 shows again that the impact-driven

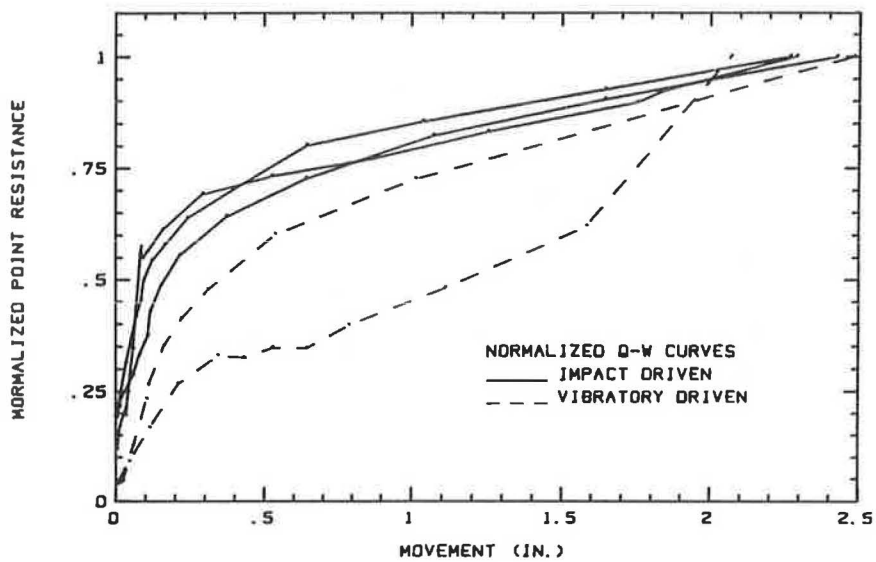

FIGURE 14 Normalized point load transfer curves.

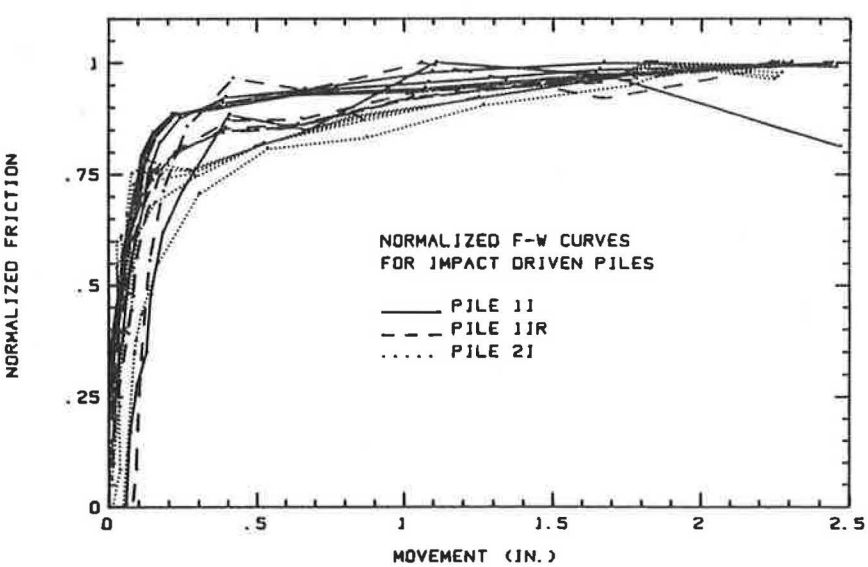

FIGURE 15 Normalized friction transfer curves for impact-driven piles.

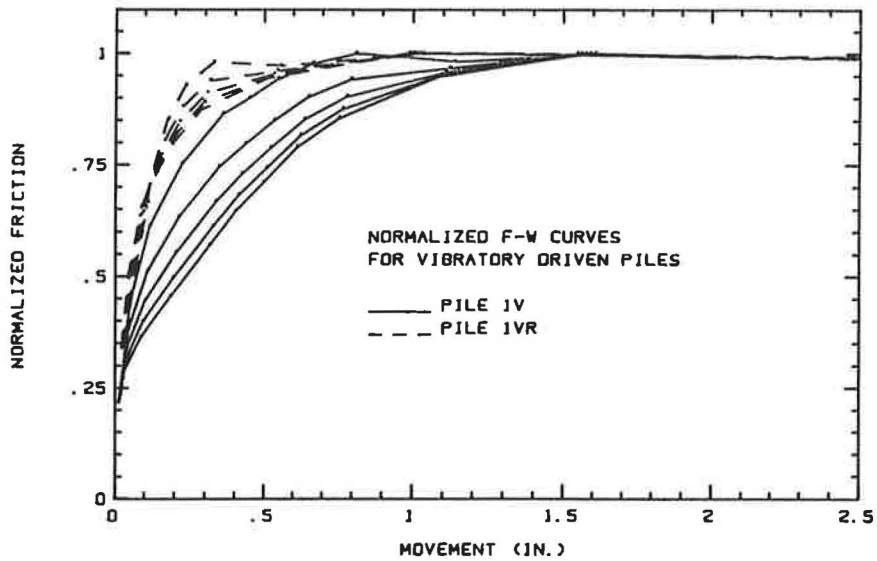

FIGURE 16 Normalized friction transfer curves for vibratory-driven piles.

piles are very consistent in their responses and that no change in behavior occurs between initial loading and reloading. However, Figure 16 shows that the vibratory-driven pile exhibits a great change in behavior between initial loading and reloading. The five curves for the initial loading have a much softer initial response than the reloading curves. The initial loading curves also become softer as the depth increases, whereas the reload curves become stiffer as the depth increases. The reloading curves exhibit a pattern that matches the impact-driven piles very well.

Effect of Time

Piles 1I and 1V were tested about 31 days after driving and then retested about 65 days after driving. The plots of ultimate load versus time for two criteria are shown in Figures 17 and 18. The trend given by those two figures does not allow us to conclude that there is an increase in capacity versus time. Indeed, Figure 17 shows an increase in stiffness, but Figure 18 shows a decrease in capacity for the vibratory-driven piles; for the impact-driven piles, Figure 17 shows an increase while Figure 18 shows a slight increase. At Lock and Dam 26, where impact-driven H piles were also load tested (*6*), the capacity obtained in the load test was 67 percent higher than the capacity predicted by the wave equation method, on average. This could have been due to a 67 percent average gain in capacity of the piles between the time of driving and the time of the load test (1 week). Note that the sand at Lock and Dam 26 had an average of 7.5 percent passing the No. 200 sieve and a blow count averaging 30 bpf, while the sand at Hunter's

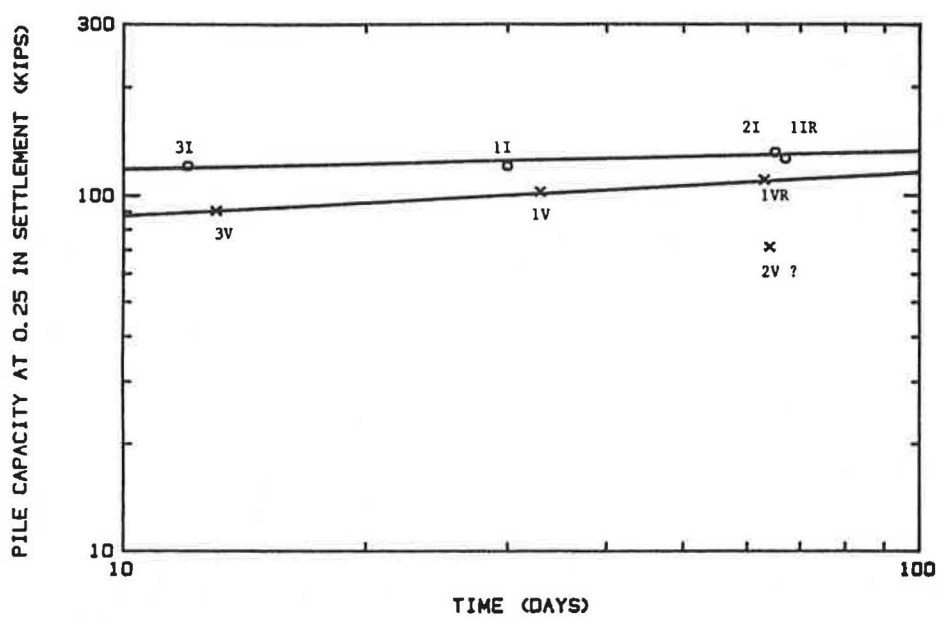

FIGURE 17 Pile capacity at 0.25 in. settlement versus time.

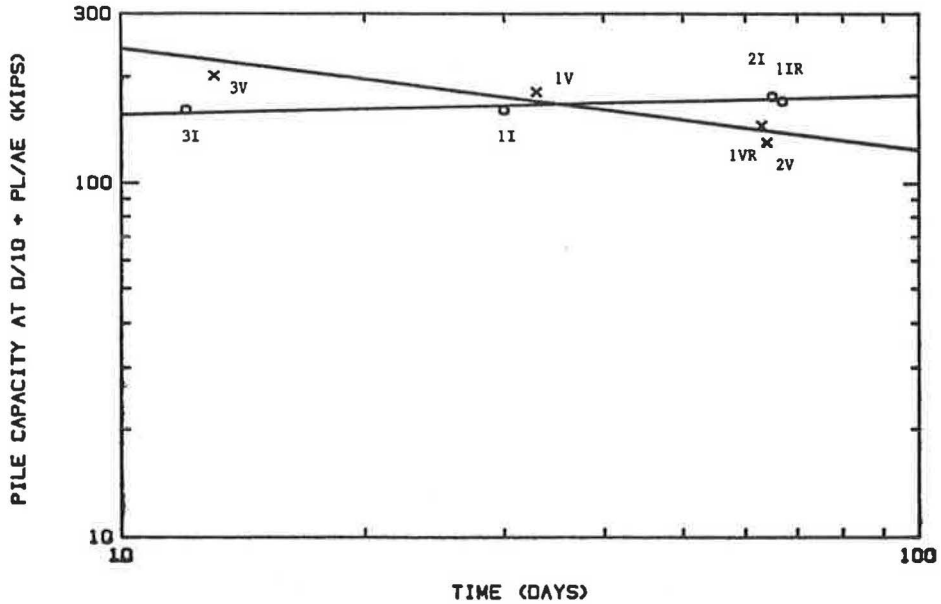

FIGURE 18 Pile ultimate capacity versus time.

Point had 0 percent passing the No. 200 sieve and a blow count averaging 15 bpf.

In the case of Hunter's Point, several factors influence the change of capacity, one of which is the effect of time. The others include the influence of soil heterogeneity and the influence of the first load test on the second load test. In order to isolate the effect of time, one solution would be to use low-strain testing to obtain the variation of stiffness versus time. Another solution would be to use a series of load tests more closely spaced in time, performed on the same pile over a longer period of time (e.g., 1 day, 4 days, 15 days, 40 days, 100 days).

CONCLUSIONS AND RECOMMENDATIONS

The main conclusions to be drawn from this study are the following:

1. Compared to impact driving, vibratory driving of piles leads to approximately the same maximum load at large movements, to a large scatter in this maximum load from one pile to the next, and to a larger movement at working loads. This larger movement was only 0.25 in. and may not require a reduction in allowable load; however, the scatter in the maximum load may require a higher factor of safety for the same risk level and therefore a lower allowable load.
2. The load distribution is influenced greatly by the driving process. For the piles in this study, impact driving led to a point resistance that was 51 percent of the total load at maximum loading, compared to 13 percent for vibratory driving. The load transfer curves are also affected by the driving process. Vibratory driving led to load transfer curves that required much larger movements to reach maximum loading.
3. The effects of vibratory driving listed above are lessened upon reloading of the pile. Upon reloading, a vibratory-driven pile carries a larger percentage of the load in point resistance, and the load transfer curves take on the same shape as the impact-driven piles. It would therefore seem desirable to have a vibratory hammer that can switch to an impact hammer and impart a few seating blows at the end of the vibro-driving sequence.
4. The data show that, in this relatively loose clean uniform sand, there is a trend for impact-driven piles towards a slight increase in capacity versus time. For vibratory-driven piles however, the data does not show any clear trend.
5. The piles encountered very easy driving, and the time required to driven the piles was the same for the impact and vibratory hammer.

ACKNOWLEDGMENTS

This project was sponsored by the U.S. Army Engineer Division, Lower Mississippi Valley, and monitored by the U.S. Army Engineer Waterways Experiment Station. Frank Weaver and Rich Jackson of LMVD and Britt Mitchell of WES are thanked for their valuable comments and support.

REFERENCES

1. E. S. Ng, J.-L. Briaud, and L. M. Tucker. *Pile Foundations: The Behavior of Piles in Cohesionless Soils*, Report FHWA-RD-88-080. FHWA, U.S. Department of Transportation, 1988.
2. E. S. Ng, J.-L.Briaud, and L. M. Tucker. *Field Study of Pile Group Action in Sand*. Report FHWA-RD-88-081. FHWA, U.S. Department of Transportation, 1988.
3. L. M. Tucker and J.-L. Briaud. *Axial Response of Three Vibratory*

and Three Impact Driven H Piles in Sand. Miscellaneous Paper GL-88-28. U.S. Army Engineer Waterways Experiment Station, Vicksburg, Miss., 1988.
4. A. H. Hunter and M. T. Davisson. Measurements of Pile Load Transfer. In *Performance of Deep Foundations*, Report STP 444, American Society for Testing and Materials, New York, 1969, pp. 106–117.
5. F. Rausche, G. G. Goble, and G. E. Likins. Dynamic Determination of Pile Capacity. *Journal of Geotechnical Engineering*, ASCE, Vol. 3, No. 3, 1985, pp. 367–387.
6. L. M. Tucker and J.-L. Briaud. *Analysis of the Pile Load Test Program at the Lock & Dam 26 Replacement Project*. Miscellaneous Paper GL-88-11. U.S. Army Engineer Waterways Experiment Station, Vicksburg, Miss., 1988.
7. D. M. Holloway. *Dynamic Monitoring Program Results, FHWA Vibratory Hammer-Pile Testing, Hunter's Point, California*. Report to Geo/Resource Consultants, 1987.

Publication of this paper sponsored by Committee on Foundations of Bridges and Other Structures.